An Investigation on Corrosion Inhibition Potential of Thiourea-Zn^{2+}-Glycine System: Sulphuric Acid Corrosion on Mild Steel

M.B. Geetha[1], S. Venkatesa Prabhu[2], and S. Rajendran[3]

[1]Department of Chemistry, St.Michael College of Engineering and Technology, Kalayarkoil, India.

[2]Department of Chemical Engineering, Addis Ababa Science and Technology University, Addis Ababa, Ethiopia.

[3]Department of Chemistry, St.Antony's College of Arts and Sciences for Women, Dindigul, India.

Abstract:

In the present study, the inhibition potential of the combination of the compounds, thiourea-Zn^{2+}-glycine on mild steel (MS) corrosion was investigated. Predetermined corrosion on MS was carried out H_2SO_4 at pH 4. The examinations on study was made using different gravimetric and conventional techniques including surface morphology, polarization, AC impedance SEM, AFM, UV, and fluorescence. The impedance measurements confirmed the polarization behavior of the corrosion products. In addition, the polarization profile showed that the inhibitor behaves as mixed type with more pronounced cathodic effect. The observed corrosion data indicated that the inhibition of MS corrosion due to adsorption of the inhibitor molecule on the metal surface that helps to minimize the corrosion. Form the inference, the combination of the inhibitors contained, 100 ppm of thiourea, 25 ppm of Zn^{2+} and 250 ppm of glycine showed very good inhibition efficiency on MS corrosion.

Keywords: Corrosion Inhibition, Mild steel, H_2SO_4, Thiourea, Polarization, SEM, AFM.

1. Introduction

Mild steel (MS) has a quite potential as wide applicable metal because of its relatively low price. It has appreciable material properties that acceptable for many applications such as boilers, water pipe lines, machine parts, and for chemical storage bins. Nevertheless, mild steel is generally interacts with sulphuric acid and gets affected. Since sulphuric acid are used in different industries for several purposes like pickling, cleaning, and descaling. So, the possibility of its interaction for corrosion with MS is seems to be more common. Corrosion of MS with sulphuric acid creates lot of technical & economic issues in different process industries. Henceforth, different researchers are showing quite interest for identifying an effective inhibitors for such kind of corrosion on MS. In order to meet the needs of various industrial requirements with respect to corrosion inhibition of MS, the serious investigations for this issue are gaining immense important. In the present study, an investigation was carried out to examine the potential of inhibitor property of combined compounds, thiourea (TU) $[CS(NH_2)_2]$, Zn^{2+}, and glycine (NH_2-CH_2-COOH). The combination of compounds was used as inhibitor against corrosion on MS by sulphuric acid. The examination on inhibitor performance using the combination thiourea-Zn^{2+}-glycine was characterized by different techniques such as weight loss, AC impedance, polarization, FT-IR, UV absorption, fluorescence, SEM-EDAX, and AFM.

2. Material and Methods

2.1 Material

The samples of MS sheets (1×4×0.2 cm) was used in this study is known to be has composed with 0.026%-S, 0.06%-P, 0.4%-Mn and 0.1%-C, and rest-Fe. The samples were polished to a mirror finish followed by subjected to degrease using trichloroethylene. Further, the samples were washed with distilled water and allowed to dry. The experiments were carried out using H_2SO_4 prepared with a pH value 4.

2.2 Experimentation for Corrosion Studies

1 g of TU was dissolved in doubled distilled water and made up to 100 ml in a standard flask. 1 ml of this solution was diluted to give 100 ml of 100 ppm of TU. For glycine solution, 1 g of glycine was dissolved in doubled distilled water and made up to 100 ml in a standard flask. 1 ml of this solution was diluted to give 100 ml of 100 ppm of Glycine. For Zn ion, the zinc sulphate solution was prepared as follows. 4.4 g of zinc sulphate was dissolved in double distilled water and made up to 1 liter. 2.5 ml of this solution was diluted to give 100 ml of 25ppm of $ZnSO_4$ solution. The different corrosion environments were prepared as per the predetermined concentrations of sulphuric acid preparations. A ddifferent set of solutions of inhibitors like 100, 150, 200, and 250 ppm was prepared while keeping the concentration of Zn^{2+} as 25 ppm and maintained the pH as 4. The corrosion studies were carried out for 24 h.

2.3 Characterization Studies

2.3.1 Determination of Weight Loss

A weigh balance (Shimadzu AY62) was used to determine the weights loss measurement of the sample. Determination of weight loss was carried out by immersing the MS plate samples in 100 ml H_2SO_4. Clean glass hooks were used for holding the samples in the glass beaker. The beaker contained 100 ml of H_2SO_4 adjusted with pH 4. Different predetermined concentrations of inhibitor solutions were added to the beaker. The experiment was carried out at room temperature (303K). After 24 h the MS strip samples were taken out and washed in tap water followed by distilled water. Then, they were dried, and weighed accurately.

2.3.2 Synergism effect of corrosion inhibitors

Synergism parameter [denoted (S_1)] has been used to find out the synergistic effect existing between two inhibitors. Synergism parameter (S_1) can be calculated using the relationship given in Eq. (1).

$$\text{Synergism parameter } (S) = \frac{1-\theta_{1+2}}{1-\varphi_{1+2}} \quad \ldots\ldots (1)$$

Where, $\theta_{1+2} = (\theta_1+\theta_2) - (\theta_1\theta_2)$, θ_1 refers to surface coverage of inhibitor for thiourea, and Zn^{2+}, θ_2 denotes surface coverage of inhibitor for glycine, $_{1+2}$ refers to combined inhibition efficiency of inhibitor thiourea and Zn^{2+}-glycine.

2.3.3. Polarization studies

Polarization studies carried out using an electrochemical impedance analyzer (A CHI, 660A model). It was used to record both polarization and AC impedance measurements. In this case, three electrode cell assemblies were used. MS was used as the working electrode. On other hand, a saturated calomel electrode was used as a reference electrode. Platinum was used as a counter electrode. Polarization profiles were recorded after performing iR compensation. From the observations, the corrosion parameters such as Tafel slopes (anodic slope b_a and cathodic slope b_c), corrosion current (I_{Corr}) and corrosion potential (E_{Corr}) values were calculated. During the polarization studies, the scan rate (V/s) was fixed as 0.005; hold time at E_f (s) was fixed at zero, and quiet time (s) was set to 2.

2.3.4 AC impedance studies

For AC impedance study, the same instrument utilized for polarization was used. The cell set-up was fixed as same as that had been used for polarization investigation. The real part and imaginary part of the cell impedance were measured in ohms at various frequencies. A time interval of 5 to 10 min was set to the system to attain its open circuit potential. The values of charge transfer resistance ($_t$) and the double layer capacitance ($_{dl}$) were also calculated as per the procedure.

2.3.5 Studies on Surface Examination.

The MS specimens were kept immersed in various test solutions for one day. Then they were dried. Due to the interaction between metal surface and reaction soltion film may be foemed on the metal surface. The nature protective film formed on the surface of the metal specimen was analyzed. This was carried out by surface analytical techniques such as FT-IR, SEM cupled with EDAX, and AFM.

2.3.5.1 FT-IR Analysis

FTIR spectra of pure TU, glycine and 100 ppm of TU, 25 ppm of Zn^{2+} and 250 ppm of glycine system were recorded using a spectrophotometer (Perkin-Elmer 1600). After predetermined time of treatment, the film obsereved from the MS surface was carefully removed and mixed thoroughly with KBr (1%). Further, this was made into pellets followed by FT-IR spectra amnalyis were employed.

2.3.5.2 UV-Visible Absorbance Spectrurm and Fluorescence Spectrum

UV–visible absorption and Fluorescence spectrum analysis was carried out on the MS samples after the corrosion treatment. This analysis was carried out at before and after addition of the inhibitors. UV spectra measurements were carried out using an UV Spectord S-100 analytic Jena spectrophotometer. In order to analyze fluorescence prosperity of the treated samples, a fluorescence spectrum analysis was conducted using Glaxo F-6300 Spectro-fluorimeter.

2.3.5.3 SEM-EDAX Studies

The surface morphology investigation on treated MS was assessed. A scanning electron microscopy (SEM) (HITACHI S-3000H SEM) and the corresponding EDAX spectrum studies were also carried out for detecting the various elements presence on the surface.

2.3.5.4 Atomic Force Microscopy

Atomic Force Microscopy characterization is a powerful technique for the gathering of roughness statistics from a variety of surfaces. For better understanding of the surface morphology of the MS, Atomic Force Microscopy (AFM) (SPM 2100 AFM) was used.

3. Result and Discussion

3.1 Weight loss Measurements

Weight loss Measurement is the basic method for inhibition assessment. After treatment with different concentrations of inhibitors the MS specimens were subjected to assess the weight loss. The observed results are tabulated in Table 1. In terms of weight loss, inhibition efficiency was calculated by the following Eq. (2).

$$(IE)\ \text{Inhibition Efficiency} = 1 - \frac{W_2}{W_1} \times 100\ \% \ldots\ldots\ldots (2)$$

Where, W_1 and W_2 are corrosion rate in the absence and presence of inhibitors, respectively. The corrosion rate (CR) also can be calculated using the formula (3) through weight inferences.

$$CR\ (\text{Millimetre per year}) = 87.6\ W/DAt\ mm/y \ldots\ldots\ldots\ldots (3)$$

Where, W = weight loss in mg, D = 7.87 g/cm^3, A = surface area of the specimen (10 cm^2), t = 24 h. The results obtained from the experimental studies for weight loss studies for at different TU concentrations in the absence and presence of Zn^{2+} for the MS corrosion in H_2SO_4 (one-day treatment) are given in table 1. It was found that TU well inhibits the MS corrosion. As per the inference, WL increases with concentration of TU increases. At fixed concentration of Zn^{2+} (25 ppm) with TU, the WL increased with increase in the TU concentration. At the experiment, with 25 ppm Zn^{2+} without TU, the low IE was observed (10 %). On other hand, 250 ppm of TU without Zn^{2+} showed 55 % of IE. It was observed that highest value of IE 82% when the treatment was carried at combination of 250 ppm TU and 25 ppm Zn^{2+}.

Table 1. The corrosion rate (CR) and inhibition efficiency (IE) for the different combinations of TU and Zn^{2+}

T J (ppm)	Without Zn^{2+}		With Zn^{2+} (25 ppm)	
	IE (%)	CR (mm/y)	IE (%)	CR (mm/y)
0	-	0.1947	10	0.1762
50	38	0.1205	55	0.0881
100	45	0.1113	65	0.0672
150	48	0.1020	74	0.0510
200	50	0.0974	80	0.0394
250	55	0.0881	82	0.0348

Table 2. Corrosion rate (CR) and inhibition efficiencies (IE) of different combinations of TU+Zn^{2+}-Glycine system

TU (ppm)	Zn^{2+} (ppm)	Glycine ppm	Corrosion Rate (mm/a)	I.E (%)
0	0	0	0.1947	---
0	25	0	0.1762	10
100	25	50	0.02783	80
100	25	100	0.0394	82
100	25	150	0.0324	83
100	25	200	0.0278	86
100	25	250	0.0185	90

In order to achieve developed IE at lower concentration levels of binary inhibitor system, the influence of another inhibitor, glycine, at various concentrations was investigated. The combination of glycine with TU and Zn^{2+} at different concentrations and the resulted IE values on MS were examined and presented in Table 2. As per the observed results, it was found that when the concentration of the glycine in TU-Zn^{2+} solution increased and the value of IE also were observed to be increased. The concentration of inhibitor combination, 100ppm: TU, 25ppm: Zn^{2+}, and 250ppm: Glycine showed 90% of IE. Hence, this ternary combination of inhibitor concentration was identified for better IE than the use of individual inhibitor [1]. The results indicate

that the synergistic effect exists among the combination of the compounds TU, Zn^{2+} and Glycine. This synergism is responsible for increase in IE and decrease in corrosion rate [2-3].

3.2 Potentiodynamic Polarization Study

Figure 1 depicts the potentiodynamic polarization profiles of MS treated with H_2SO_4 (at pH-4, contained 100 ppm of TU, 25 ppm of Zn^{2+} and 250 ppm of glycine). The corrosion parameters are presented in Table 2. In the presence of inhibitors, the corrosion potential shifted to cathodic side (from −598mV to −660mV vs. SCE). This observation suggested that the cathodic reaction was controlled the corrosion reaction predominantly. The largest shift evidenced by this inhibitor system was 62 mV. Therefore, it ensured that this system functions as a mixed type inhibitor [4-5]. Simultaneously, in the presence of the inhibitor system, the corrosion current decreases from $2.394x10^{-6}$ A/cm^2 to1.001 x10 $^{-6}$ A/cm ^{2} and LPR value increases from 16724.9 ohm-cm^2 to 41129 ohm-cm^2. Linear Polarization Resistance (LPR) value increased with the decrease in corrosion current density indicated the adsorption of the inhibitor on the metal surface to block the active sites and inhibit corrosion. This reduces the corrosion rate with the protective film formation on the metal surface [6].

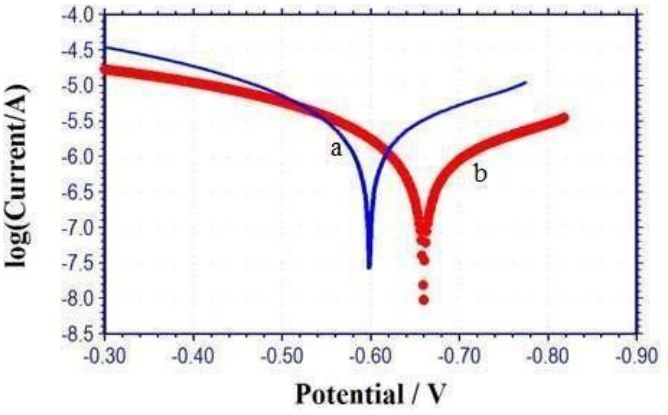

Figure. 1 The polarization profiles of MS after corrosion (a) pH−4 H_2S0_4; (b) pH 4 H_2S0_4+TU (100 ppm) + Zn^{2+} (25 ppm) + Glycine (250ppm)

Table 2. Corrosion parameters of MS immersed in H_2SO_4 solution at pH-4 in the absence and presence of inhibitor system TU (100 ppm) and Zn^{2+} (25 ppm)-Glycine (250 ppm) obtained by polarization method

TU ppm	Zn^{2+} ppm	Glycine ppm	E_{corr} mV vs. SCE	b_c mV/decade	b_a mV/decade	LPR ohm cm^2	I_{corr} A/cm^2
0	0	0	−598	205	167	16724.9	$2.394x10^{-6}$
100	25	250	−660	219	167	41129.0	$1.001x10^{-6}$

3.3 Analysis of AC impedance spectrum

The AC impedance spectrum studies on treated MS with H_2SO_4 solution at pH-4 containing 100 ppm of TU, 25 ppm of Zn^{2+} and 250 ppm of glycine is presented in Figure 2 (Nyquist plots). For the same studies, the Bode plots are given in Figure 3. The AC impedance parameters, charge transfer resistance (R_t) and double layer capacitance (C_{dl}) are shortened in Table 3. From the table 3, it is obvious that the addition of inhibitors, R_t value raises from 4857 ohm-cm^2 to 12680 ohm-cm^2 and the C_{dl} decreases from $3.9489x10^{-9}$ F/cm^2 to $1.5126x10^{-9}$ F/cm^2. This decrement in C_{dl} and increment in R_t confirms that the MS dissolution is retarded due to adsorption of inhibitors on the metal surface [7-8]. This can be vindicated by the raise in impedance value from 3.792 to 4.420 log (z/ohm).

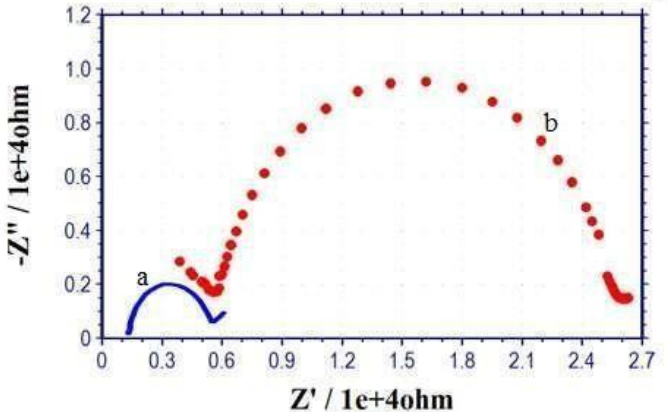

Figure 2. AC impedance spectra (Nyquist plots) of MS after treatment. (a) pH-4 H_2S0_4; (b) pH-4 H_2S0_4+TU(100 ppm)+Zn^{2+} (25 ppm)+glycine (250ppm)

Figure 3 AC impedance spectra (Bode plots) of MS treated at various test solutions (a) pH-4 H_2SO_4; (b) pH-4 H_2S0_4+TU (100 ppm) + Zn^{2+} (25 ppm) + Glycine (250 ppm).

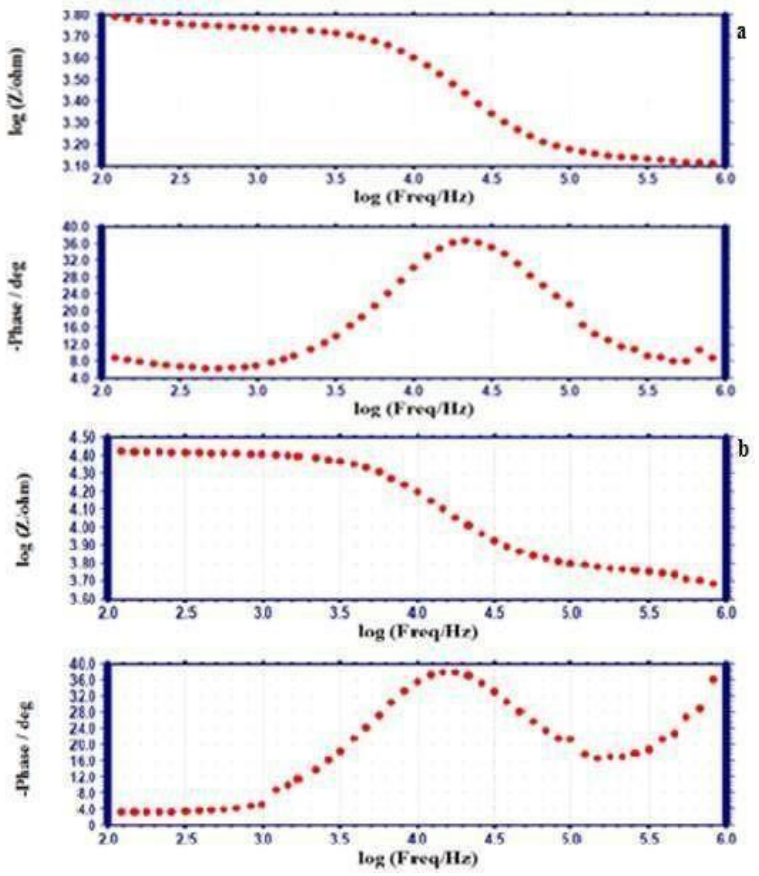

Table 3. Corrosion parameters of MS immersed in H_2SO_4 solution at pH-4 in the absence and presence of inhibitor system (TU-Zn^{2+}-Glycine) obtained by AC impedance method

System	Nyquist plot		Bode plot
	R_t ohmcm^2	C_{dl} F/cm^2	Impedance value log (z/ohm)
H_2SO_4 solution at pH-4	4857	3.9489×10^{-9}	3.792
H_2SO_4 solution at pH-4 + 100 ppm TU + 25 ppm Zn^{2+} + 250 ppm of Glycine.	12680	1.5126×10^{-9}	4.420

3.4 UV–Visible Absorption Analysis

The UV-Visible absorption spectrum of an aqueous solution containing TU-Fe^{2+} (Figure 4) showed an absorbance of 0.026 at the wave length of 392 nm which corresponds to Fe^{2+}-TU complex. When glycine was added to the above mentioned solution, the band of an absorbance 0.559 observed to shift at 304 nm which is shown in the Figure 4.49 (b). There was a quite deviation in the maximum absorbance values and their intensities. This shift of the position for maximum absorbance and change in value of wavelength indicates the formation of a complex between two species in solution [9]. This peaks corresponds to TU-Fe^{2+} and glycine-Fe^{2+} complex. This complex might be adsorbed on the metal surface and prevented the metal from further corrosion as a barrier [10-11].

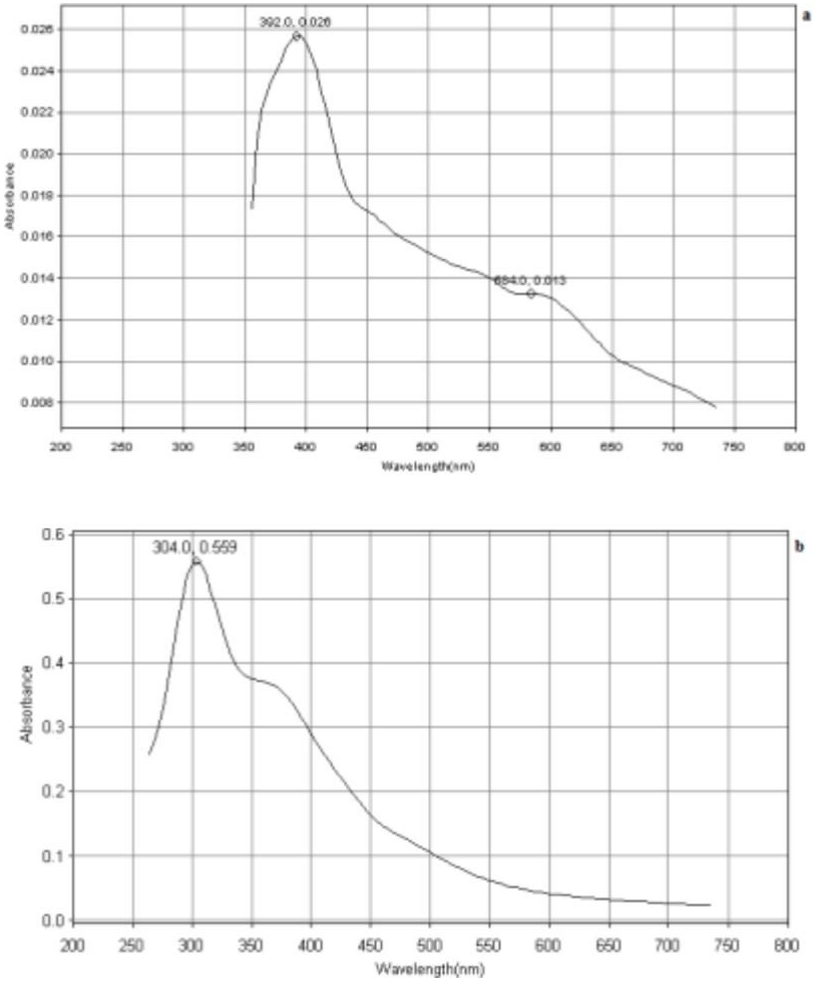

Figure 4. UV absorption spectra of solutions (a) TU-Fe^{2+} complex in solution; (b) TU-Fe^{2+}, Glycine-Fe^{2+} complex in solution

3.5 Fluorescence spectrum Analysis

The emission spectrum (λ_{ex}−300 nm) of the inhibitor solution contain TU, Fe^{2+} and glycine presented in Figure 5 a. It showed a peak at 396.5 nm with intensity 57.753 mV. The emission spectrum (λ_{ex}−300 nm) of the film produced on the metal surface after immersing in MS in the solution had 100 ppm TU, 25 ppm Zn^{2+}, and 250 ppm glycine (Figure 4. b) showed a peak with fluorescence intensity (I_o = 56.287 mV) at 400 nm (λ_{max}). Both the peaks confirmed the presence of TU-Fe^{2+} and glycine-Fe^{2+} complex on the metal surface. The decrease in emission

intensity might be due to the fact that electronic transition was difficult in the solid state film. It was found that only one peak was obtained. Hence, nature of the complex can be said as highly symmetric [12-13].

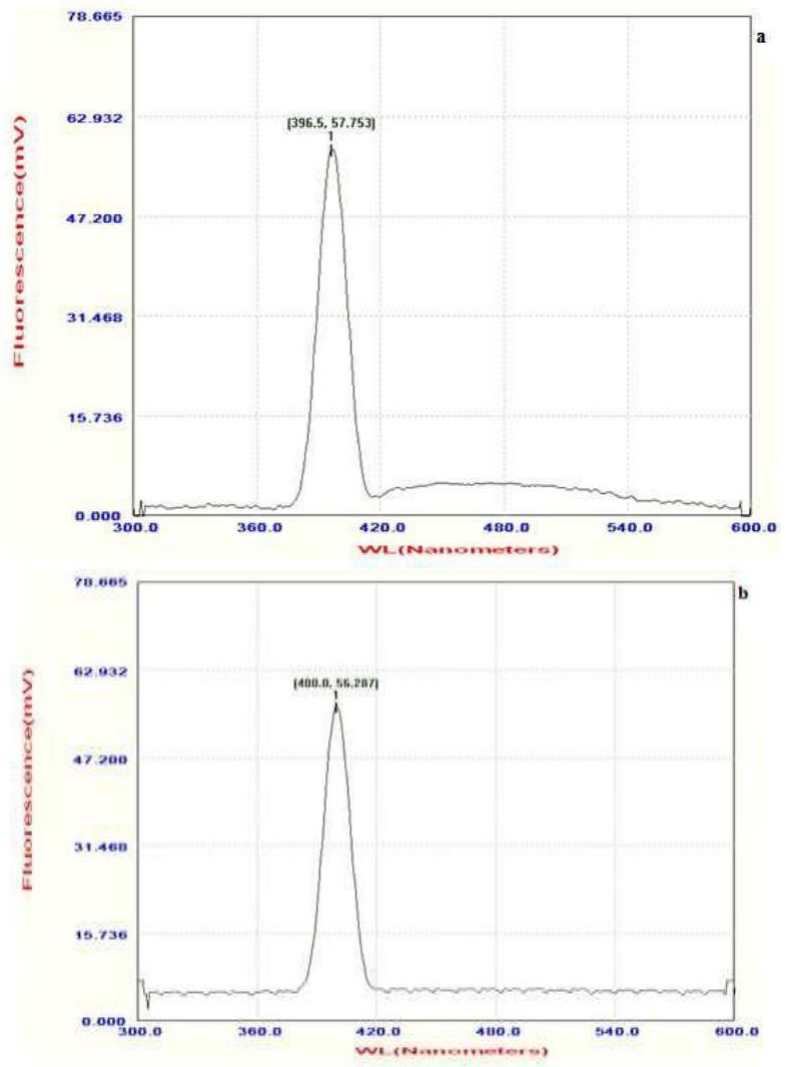

Figure 5 Fluorescence spectra of solutions (a) TU-Fe^{2+}-Glycine complex in solution; (b) Film formed on the metal surface after immersion in the solution containing 100 ppm TU, 25 ppm Zn^{2+} and 250 ppm Glycine

3.6 FT-IR Analysis

Figure 7 shows the FT-IR spectra (solubilized at KBr) of pure TU, pure glycine, and the combination of predetermined concentrations of TU-Zn^{2+}-glycine. It was inferred from the figure that The C=S stretching frequency was emerged at 1609.30 cm^{-1}. The N–H stretching and bending frequency emerged respectively at 3381.67 cm^{-1} and 1412.85.47 cm^{-1}. The C–N stretching and vibration frequency emerged at 1466.6 cm^{-1} and 1082.57 cm^{-1}. The C=O, C−N and N−H stretching frequency emerged, respectively at 1587cm^{-1}, 1125.03 cm^{-1} and 3092.23 cm^{-1} in the glycine FTIR spectrum (Figure 6 b).The FTIR spectrum of the film formed on the metal surface following immersion in H_2SO_4 solution at pH-4 having 100 ppm TU, 25 ppm Zn^{2+} and 250 ppm glycine was shown in Figure 8. From the spectra, it cleared that the C=O stretching frequency shifted to 1614.71 cm^{-1}.

The N−H stretching frequency shifted to 3436.04 cm^{-1}. The C=S stretching frequency shifted to 1590.36 cm^{-1}. The C–N stretching frequency shifted to1383.56 cm^{-1} and the C–N vibration frequency appeared at 1018.21 cm^{-1}. The peak observed at 765.41 cm^{-1} indicated stretching frequency due to Zn-O. This shift in frequencies implies that TU and glycine coordinated with Fe^{2+}. This resulted because of the formation of TU-Fe^{2+} complex and glycine-Fe^{2+} complex [14-16].

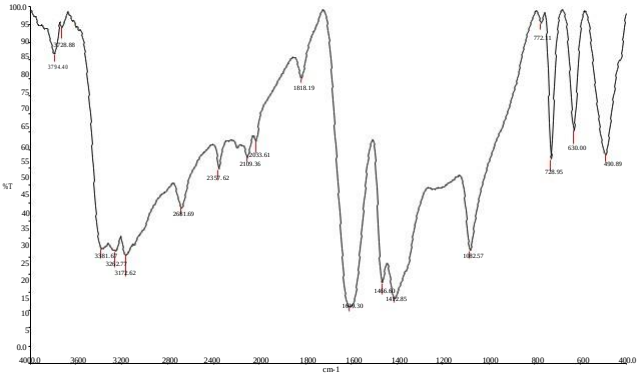

Figure 7. FTIR Spectrum of film formed on the metal surface after immersion in H_2SO_4 solution at pH-4 containing with pure TU

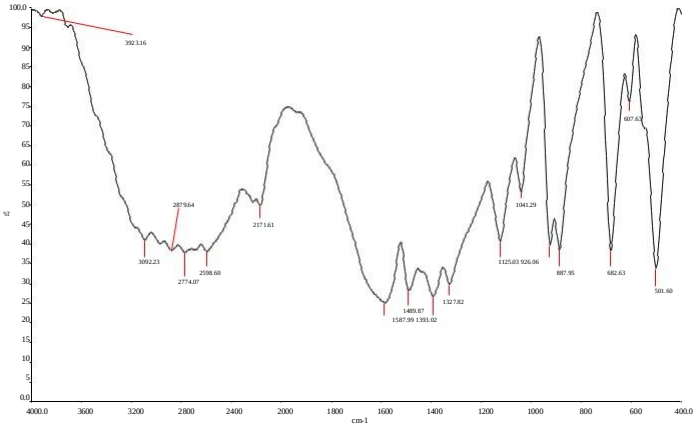

Figure 8. FTIR Spectrum of film formed on the metal surface after immersion in H_2SO_4 solution at pH-4 containing with pure glycine

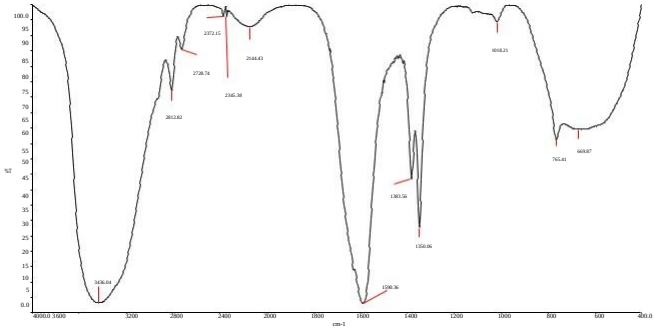

Figure 9. FTIR Spectrum of film formed on the metal surface after immersion in H_2SO_4 solution at pH-4 containing TU (100 ppm) and Zn^{2+} (25 ppm)+glycine (250 ppm)

3.7 SEM Analysis of Metal Surface

The polished MS surface (control) SEM micrographs are given in Figure 10. It showed the smooth metal surface without any inhibitor complex formation or corrosion products on the metal surface. The SEM micrographs of MS surface after immersed in H_2SO_4 solution at pH-4 in the absence of inhibitor are presented in Figure 10 (c, d). The observation showed a quite unevenness of the metal surface due to the corrosive

environment. There was a formation of different corrosion products (Iron oxides) and pits on the MS surface while absence of the inhibitor. The SEM images of treated MS surface (at 100 ppm TU, 25 ppm Zn^{2+} and 250 ppm of glycine) are given in Figure 7 (e, & f). The inference from those images indicated that the rate of corrosion was diminished because of the inhibitor absorption on the metal surface forming a passive film on the metal surface. Therefore, the inhibitors, TU, Zn^{2+} and glycine depress corrosion by the protective film formation on the metal surface which was responsible for corrosion inhibition [17-19].

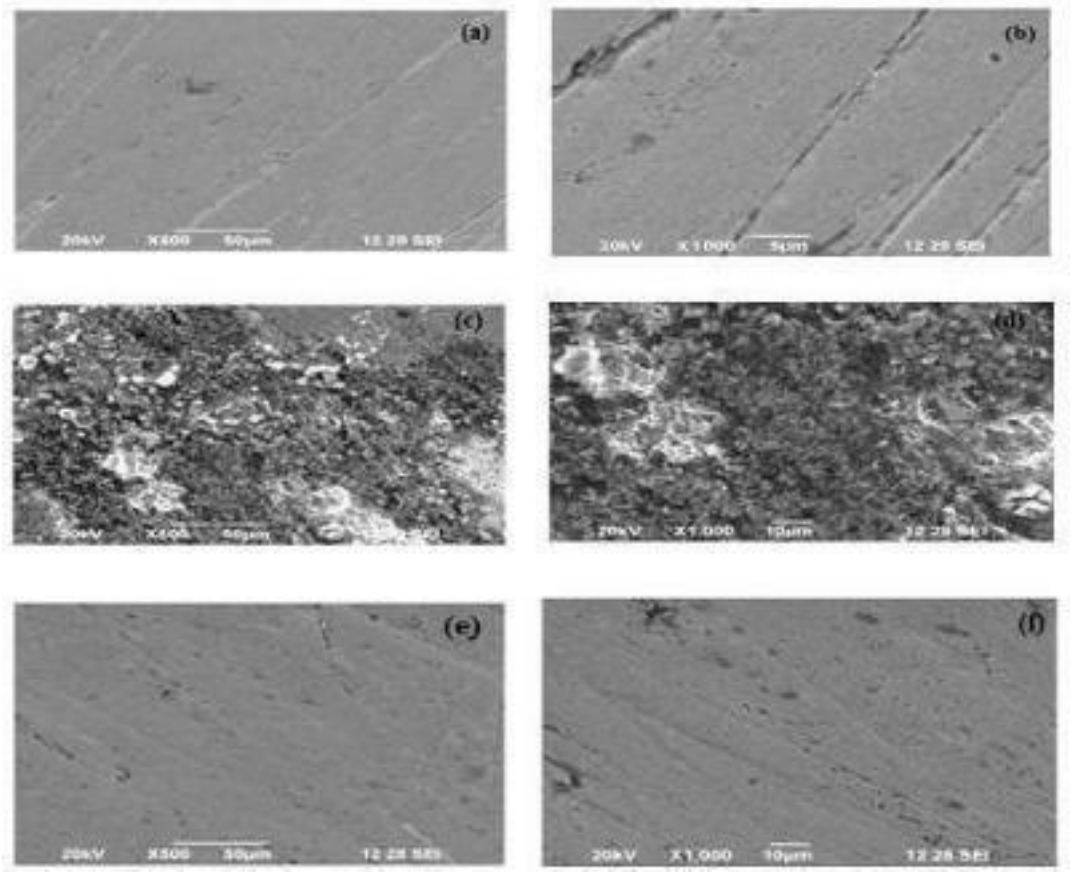

Figure 10. SEM micrographs of MS surface with different magnifications. (a) & (b) before immersion in pH-4 H_2SO_4; (c) & (d) after one day immersion in pH-4 H_2SO_4; (e) & (f) after one day immersion in pH-4 H_2S0_4+ TU (100 ppm)+Zn^{2+} (25 ppm)+Glycine (250 ppm).

3.8 Energy Dispersive Analysis of X-Rays

The EDAX spectra are given in Figure 8. In the case of polished metal, the iron peak was observed to be very high. When the EDAX experiments on treated MS showed the diminished intensity of Fe-peak. This was due to corrosion and corrosion products. The Fe-peak intensity was getting increased in the existence of inhibitors. This was resulted because of the inhibitors adsorption restricted corrosion. The other peaks for Zinc and Nitrogen were also observed in this case [20].

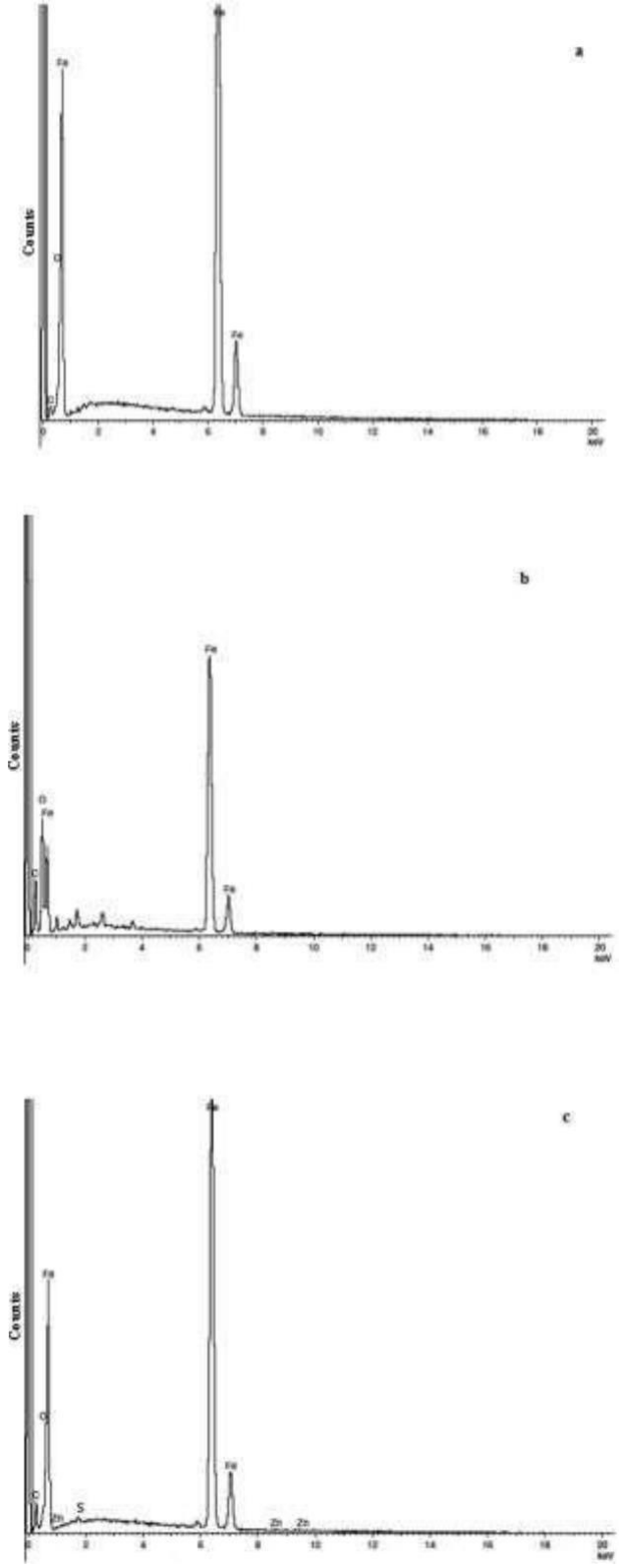
a
Counts
Fe
O
Fe
b
Counts
O
Fe
Fe
c
Counts
Fe
O
Fe
S
Zn
Zn

Figure 11. EDAX Spectrum of MS surface (a) before immersion in pH-4 H_2SO_4; (b) after one day immersion in pH-4 H_2SO_4; (c) after one day immersion in pH-4 H_2SO_4+TU (100 ppm)+Zn^{2+} (25 ppm)+Glycine (250 ppm).

3.9 Atomic Force Microscopy Characterization

The three dimensional and two dimensional AFM images of the polished MS before treatment and corroded MS after treatment and after treatment in the presence of inhibitors are shown in Figures 9, respectively. From the AFM studies, the average roughness (R_a), root mean square roughness (R_q) and maximum peak-to-valley height (P-V) value for engrossed in the different environmental conditions are given in

table 4. The values of R_q, R_a and P-V height for the polished MS surface were observed to be 26.351 nm, 21.327 nm and 129.754 nm, respectively. It shows a more homogeneousness of the surface. As a result of the atmospheric corrosion the slight roughness was noted on the polished MS surface. While the values of R_q, R_a and P-V height for the corroded MS surface (at immersed in H_2SO_4 solution at pH-4) were found to be 152 nm, 132 nm and 584 nm, respectively. That suggests that the MS surface engrossed in H_2SO_4 solution at pH-4 had a greater surface roughness because of the corrosion. Nevertheless, in the presence of TU, Zn^{2+} and glycine smoother surface was obtained and the R_q, R_a and P-V height values were found to decreased value (38.354nm, 28.527nm, and 209.047nm respectively). The drop of these parameters value established that MS surface become smoothened due to the deposition of inhibitors on the metal surface. The surface smoothness was caused by the hard protective film formation containing TU-Fe^{2+}, Glycine-Fe^{2+}complex, and $Zn(OH)_2$ on the metal surface in that way holding back the MS corrosion [21-22].

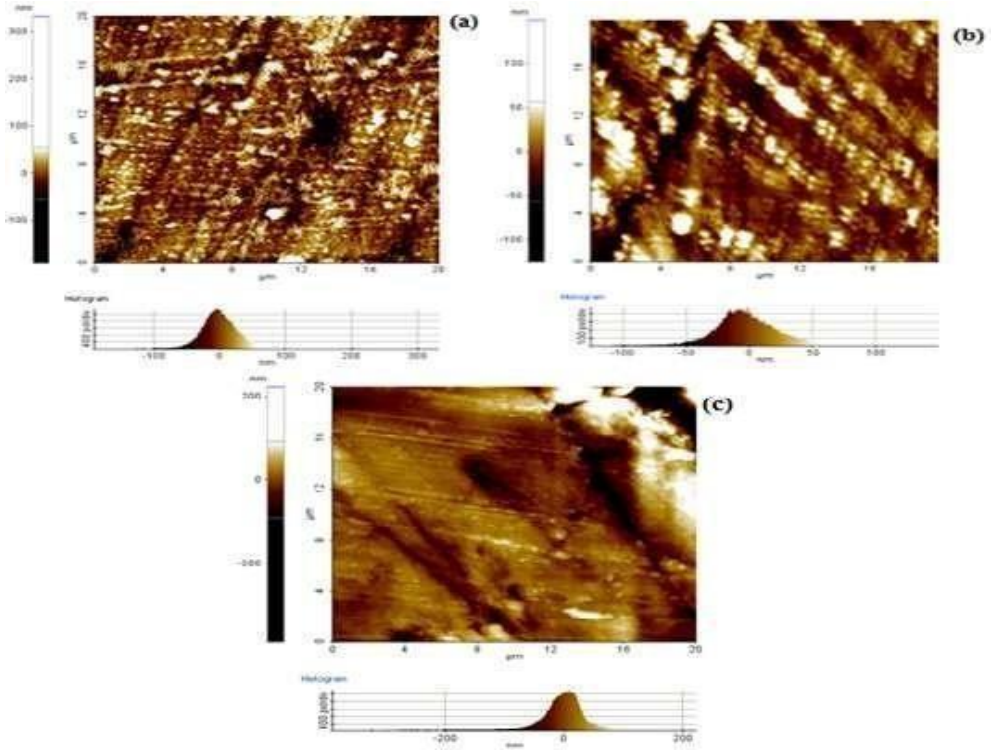

.

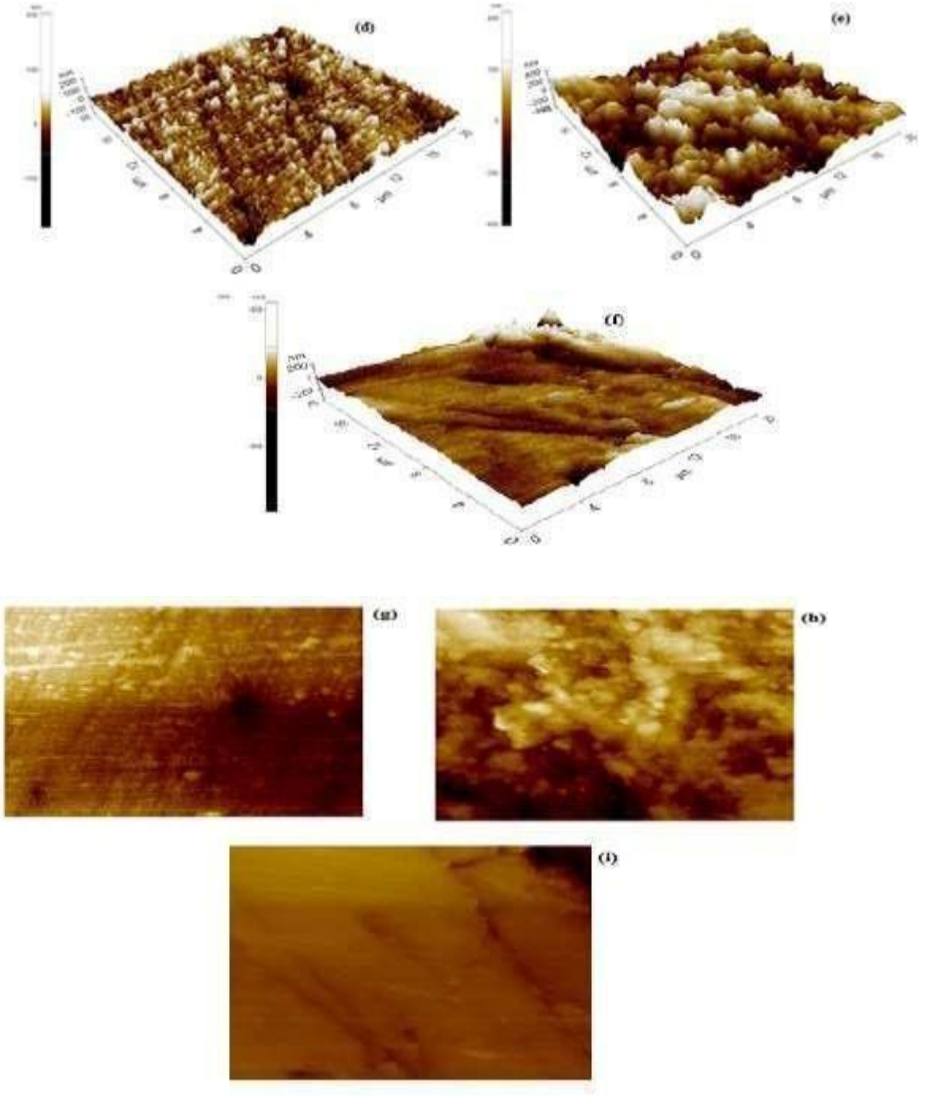

Figure 9. AFM images and Topography of the MS surface. (a) Before immersion in pH-4 H_2SO_4; (b) After one day immersion in pH-4 H_2SO_4; (c) After one day immersion in pH-4 H_2SO_4+TU (100 ppm)+Zn^{2+} (25 ppm)+glycine (250 ppm); (d) Before immersion in pH-4 H_2SO_4; (e) After one day immersion in pH-4 H_2SO_4; (f) After one day immersion in pH-4 H_2SO_4+TU (100 ppm)+Zn^{2+} (25 ppm)+glycine (250 ppm); (g) Before immersion in pH-4 H_2SO_4; (h) After one day immersion in pH-4 H_2S0_4; (i) After one day immersion in pH-4 H_2S0_4+TU (100 ppm)+Zn^{2+} (25 ppm)+glycine (250 ppm)

Table 4. AFM Data for MS surface immersed in inhibited and uninhibited environment.

Sample	Polished MS	MS immersed in H_2SO_4 solution at pH-4.

MS immersed in H_2SO_4 solution at pH-4 containing 100 ppm of TU and 25 ppm of Zn^{2+} + 250 ppm of Glycine.	RMS (R_q) Roughness (nm)	Average Roughness (R_a) (nm)	Maximum peak-to-valley height (P-V) (nm)
	26.351	21.327	129.754
	152	132	584
	38.354	28.527	209.047

4. Proposed Mechanism for corrosion Inhibition

The weight-loss study result showed that the formulation containing 100 ppm TU, 25 ppm Zn^{2+} and 250 ppm Glycine has 90% IE, in restricting MS corrosion in H_2SO_4 solution at pH-4 with a synergistic effect among TU, Zn^{2+} and glycine. Polarization study reported this formulation as a mixed type inhibitor and AC Impedance recognized the formed protective film on the surface. The protective film containing TU-Fe^{2+}, glycine-Fe^{2+} complex and $Zn(OH)_2$ was revealed by FTIR spectra analysis. Based on the above results, following corrosion inhibition mechanism can be proposed. The H_2SO_4 solution at pH-4 containing 100 ppm of TU and 25 ppm of Zn^{2+} and 250 ppm of Glycine is prepared, there might be a formulation of TU-Zn^{2+} and glycine-Zn^{2+} complex in solution. When MS was immersed in this solution, TU-Zn^{2+} and glycine-Zn^{2+} complex diffuses towards the metal surface from the bulk of the solution

- TU-Zn^{2+} and glycine-Zn^{2+} is converted into TU-Fe^{2+}, glycine-Fe^{2+} complex on the metal surface anodic sites with the release of Zn^{2+} ion.
- TU-Zn^{2+}, Zn^{2+}-Glycine + Fe^{2+} $\longrightarrow$ TU-Fe^{2+}, glycine-Fe^{2+} + Zn^{2+}
- The released Zn^{2+} reacted with OH^- to produce $Zn(OH)_2$ on the metal surface cathodic sites.
  $Zn^{2+} + 2OH^- \longrightarrow Zn(OH)_2$
- Thus the protective film consists of TU-Fe^{2+}, glycine-Fe^{2+} complex and $Zn(OH)_2$.

4. Conclusion

In order to achieve higher inhibition efficiency at lower concentration levels of 100 ppm of TU and 25 ppm of Zn^{2+}system, various concentrations of Glycine are added to this system. It is observed that when Glycine is added, the inhibition efficiency of TU- Zn^{2+} increases. The inhibitor formulation containing 100 ppm TU, 25 ppm Zn^{2+} and 250 ppm glycine showed inhibition efficiency (IE) of 90 % with a synergistic effect among TU, glycine and Zn^{2+} ions. Polarization study showed this formulation as a mixed inhibitor while AC impedance spectra confirmed the protective film formation on the metal surface. FTIR spectra exposed the presence of Fe^{2+}-TU complex, Fe^{2+}-Glycine complex and $Zn(OH)_2$ in the protective film. EDAX, UV, Fluorescent spectral data, SEM and AFM images pointed out the protective layer formation on the metal surface and its surface methodology.

5. References

1. Rao & Rao, SS 2012, Synergistic Inhibition of Corrosion of Carbon Steel by the Ternary Formulations containing Phosphonate, Zn (II) and Ascorbic Acid, Research Journal of Recent Sciences, Vol.1, no., pp.93-98.
2. Umoren S.A., Li Y., Wang F.H., 2010, Electrochemical study of corrosion inhibition and adsorption behaviour for pure iron by polyacrylamide in H2SO4, Corosion Science, vol. 52. no.5, pp - 1777 – 1786.
3. Manimaran, N , Rajendran, S , Manivannan, M & Mary, SJ 2012, Corrosion Inhibition of Carbon Steel by Polyacrylamide, Research Journal of Chemical Sciences, Vol.2, no.3, pp.52-57.
4. N. K. Gupta, M. A. Quraishi, C. Verma, and A. K. Mukherjee, “Green Schiff's bases as corrosion inhibitors for mild steel in 1 M HCl solution: experimental and theoretical approach,” RSC Advances, vol. 6, no. 104, pp. 102076–102087, 2016.
5. K. R. Ansari, M. A. Quraishi, and A. Singh, “Corrosion inhibition of mild steel in hydrochloric acid by some pyridine derivatives: An experimental and quantum chemical study,” Journal of Industrial and Engineering Chemistry, vol. 25, pp. 89–98, 2015.
6. M. Lebrini , F. Robert, C. Roos Inhibition Effect of Alkaloids Extract from Annona Squamosa Plant on the Corrosion of C38 Steel in Normal Hydrochloric Acid Medium International Journal of Electrochemical science. 5 (2010) 1698 – 1712.
7. Zhang, Gao & Zhou, GD 2007, Inhibition of copper corrosion in aerated hydrochloric acid solution by amino acid compounds, Journal of Applied Electrochemistry, Vol.37, no.4, pp.439-449.
8. Khaled, KF 2008, New Synthesized Guanidine Derivative as a Green Corrosion Inhibitor for Mild Steel in Acidic Solutions, International Journal of Electrochemical Science, Vol.3, no., pp.462-475.
9. Leelavathi, S & Rajalakshmi, R 2013, Dodonaea viscosa (L.) Leaves extract as acid Corrosion inhibitor for mild Steel – A Green approach, Journal of Materials and Environmental Science, Vol.4, no.5, pp.625-638.
10. Rose, AL , Selvarani, FR , Regis & Rose, CM 2012, Corrosion behaviour of carbon steel in river water in the presence of Lactic acid-Zn^{2+} system, International Journal of ChemTech Reserach, Vol.4, no.1, pp.157-164.

11. Thangakani, JA , Rajendran, S & Sathiabama, J 2014, Inhibition Of Corrosion Of Carbon Steel In Aqueous Solution Containing Low Chloride Ion By Glycine – Zn^{2+} System, International Journal of Nano Corrosion Science and Engineering, Vol.1, no.1, pp.50-62.
12. Abuthahir, Nasser & Rajendran, S 2014, Inhibition Of Mild Steel Corrosion By 1-(8-Hydroxyquinolin-2-Ylmethyl)Urea, European Chemical Bulletin, Vol.3, no.1, pp.40-45.
13. Gunasekaran, G , Natarajan, R & Palaniswamy, N 2001, The role of tartarate in the phosphonate based inhibitor system, Corrosion Science, Vol.43, no., pp.1615-1626.
14. Srimathi, M , Rajalakshmi, R & Subhashini, S 2014, Polyvinyl alcohol–sulphanilic acid water soluble composite as corrosion inhibitor for mild steel in hydrochloric acid medium, Arabian Journal of Chemistry, Vol.7, no., pp.647-656.
15. Noreen, A , Benita, SH & Rajendran, S 2010, Inhibition and biocide actions of Sodium dodecyl sulfate-Zn^{2+} system for the corrosion of carbon steel in chloride solution, Portugaliae Electrochimica Acta, Vol.28, no.1, pp.1-14.
16. Karthik, BB , Selvakumar, P & Thangavelu, C 2013, Corrosion Behaviour of Carbon Steel in DTPMP-ST-Zn^{2+} System: An Eco-Friendly System, Research Journal of Chemical Sciences, Vol.3, no.10, pp.16-23.
17. Shanbhag, AV , Prabhu, RA , Kulkarni, GM , Kalkhambkar, RG & Venkatesha, TV 2007, Inhibitiory effects of some imines on the corrosion of mild steel in hydrochloric acid solution, Indian Journal of Chemical Technology, Vol.14, no.6, pp.584-591.
18. Patel, NS , Jauhari, S & Mehta, GN 2009, Mild steel corrosion inhibition by bauhinia Purpurea leaves extract in 1 N sulphuric acid, Arabian Journal for Science and Engineering, Vol.34, no.2, pp.61-69.
19. Mobin, M , Parveen, M & Khan, MA 2011, Inhibition of mild steel corrosion using L-tryptophan and synergistic surfactant additives, Portugaliae Electrochimica Acta, Vol.29, no.6, pp.391-403.
20. Jayasree, AC & Ravichandran, R 2013, Corrosion Inhibition Of New Class Of Substituted Benzotriazoles Onthe brass-mm55 In Artificial Sea Water, Asian Journal of Science and Technology, Vol.4, no.11, pp.212-219.
21. Devi, BS & Rajendran, S 2011, Influence of Garlic Extract on the Inhibition Efficiency of Tri Sodium Citrate, International Journal of Chemical Science and Technology, Vol.1, no.1, pp.79-87.
22. Sahayaraja, A , Rajendran, S & Sathiyabama, P 2012, Inhibition of Corrosion of carbon steel in well water by DL-Phenylalanine–Zn^{2+} system, Journal of Chemistry, Vol.2013, no., pp.1-8.